

## LETTER TO THE EDITOR

# Oxygen Tracer Diffusion in Single-Crystal CaTiO<sub>3</sub>

Isao Sakaguchi and Hajime Haneda

*National Institute for Research in Inorganic Materials, Namiki 1-1 Tsukuba, Ibaraki, 305, Japan*

Communicated by J. M. Honig, January 10, 1996; in revised form April 15, 1996; accepted April 18, 1996

Oxygen tracer diffusion in the *b* direction in single-crystal CaTiO<sub>3</sub> has been investigated in the temperature range 1121–1313 K. The diffusion coefficients determined from penetration profiles measured with secondary ion mass spectrometry (SIMS) are  $D_v = 9.9 \times 10^{-2} \exp(-384.5 \text{ [kJ/mol]/RT}) \text{ [m}^2/\text{s]}$  and  $D_{gb} = 1.8 \times 10^6 \exp(-369.2 \text{ [kJ/mol]/RT}) \text{ [m}^2/\text{s]}$ , respectively. The tailing region in the <sup>18</sup>O diffusion profile arises from twin boundaries in CaTiO<sub>3</sub>. © 1996 Academic Press, Inc.

### I. INTRODUCTION

The perovskite structure is of great importance in certain technological applications such as ferroelectrics and superconductors. Hence, defect chemistry and oxygen diffusion are vital in controlling their physicochemical properties. Consequently, the importance of understanding ion transport behavior in these materials has resulted in numerous studies of <sup>18</sup>O diffusion, employing a variety of techniques (1–8).

The ideal structure of perovskite (CaTiO<sub>3</sub>) is cubic and consists of corner-sharing TiO<sub>6</sub> octahedra that form a regular three-dimensional framework, with Ca occupying the large cuboctahedral sites. At room temperature, Ca is slightly too small for its site, causing the TiO<sub>6</sub> octahedra to tilt and rotate slightly, thereby reducing the symmetry from cubic to orthorhombic (9). This transition results in microtwinning on the major pseudocubic axes, as the structure loses symmetry on cooling through the transition temperature. The microstructure, such as twinning (10, 11) and dislocations (12) in CaTiO<sub>3</sub>, has been studied by optical and electron microscopy and plays an important role in diffusion. Oxygen diffusion in CaTiO<sub>3</sub> has been reported by Gautason and Muehlenbachs (13). However, there is no direct evidence concerning the enhancement of oxygen diffusion by these microstructures.

An investigation of <sup>18</sup>O diffusion in single-crystal CaTiO<sub>3</sub> was carried out by means of secondary ion mass spectrometry (SIMS), in order to investigate the effect of

the microstructure on <sup>18</sup>O diffusion. In this work we have studied the effect of the microstructure on <sup>18</sup>O diffusion profiles, as well as being given direct evidence by the SIMS imaging technique.

### 2. EXPERIMENTAL

Single crystals of CaTiO<sub>3</sub> were grown by the floating zone method and oriented using the X-ray technique. Samples were cut such that the diffusion direction was parallel to the *b* axis and polished using diamond paste to a 1- $\mu\text{m}$  finish. Finally samples were cut to a 3  $\times$  3  $\times$  2 mm size by using a low-speed diamond saw. The prediffusional anneal was carried out at 1373 K for 10 h in air.

Immediately after polishing and cleaning, the sample was loaded into the exchange apparatus. The system was then closed and evacuated, and enriched <sup>18</sup>O<sub>2</sub> was introduced into the manifold at 130 Torr. After diffusion anneals, the samples were quenched by rolling back the furnace and pouring water over the quartz tube. The <sup>18</sup>O<sub>2</sub> was recovered by opening the manifold to the sorption pump.

The <sup>18</sup>O diffusion profiles were measured using a SIMS (CAMECA IMS-4F) instrument with <sup>133</sup>Cs<sup>+</sup> as the primary ion, an accelerating voltage of 10 kV, and a beam current of 10 nA. To suppress the sample charging, an electron gun was used. The intensities for the negative ions (<sup>16</sup>O and <sup>18</sup>O) were monitored, and the depth of the sputtered crater was measured using a Dektak 3030 profilometer to determine the sputter rate.

The <sup>18</sup>O concentration at any sample depth was determined from the ion intensities

$$C = \frac{I(^{18}\text{O})}{I(^{18}\text{O}) + I(^{16}\text{O})}, \quad [1]$$

and each concentration profile was fitted to the equations below.

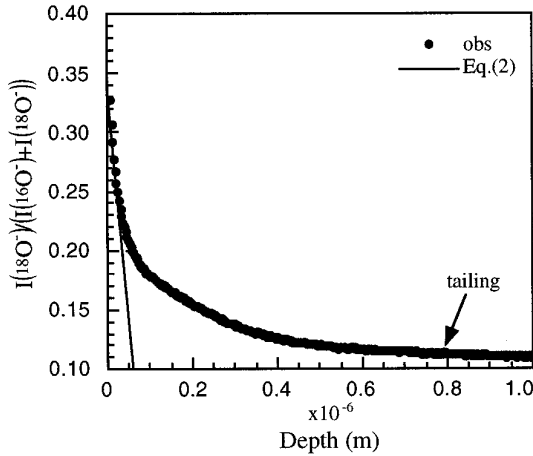


FIG. 1. Diffusion profile of  $^{18}\text{O}$  obtained from a single-crystal  $\text{CaTiO}_3$  annealed at 1121 K for 900 s. The circles show the experimental data, while the solid line is the least-squares fit to Eq. [2].

### 3. RESULTS AND DISCUSSION

A typical oxygen diffusion profile in  $\text{CaTiO}_3$  annealed at 1121 K for 900 s is shown in Fig. 1. This profile was divided into two regions: the lattice diffusion contribution near the surface, and the tailing region at the deeper side. The lattice diffusion contribution was analyzed using the equation (14)

$$\frac{C - C_{\text{bg}}}{C_s - C_{\text{bg}}} = \text{erfc}\left(\frac{x}{\sqrt{4Dt}}\right), \quad [2]$$

where  $C$  is the  $^{18}\text{O}$  concentration at depth  $x$ ,  $C_{\text{bg}}$  is the natural abundance of  $^{18}\text{O} = 0.00204$ , and  $C_s$  is the surface concentration of  $^{18}\text{O}$ . Equation [2] assumes equilibrium between the gas phase and the crystal surface and, hence, a constant  $C_s$  value. The curve calculated from Eq. [2] is shown in Fig. 1.

The tailing region in the  $^{18}\text{O}$  profile was analyzed using the equation (15)

$$\delta D_{\text{gb}} = 0.66 \left(-\frac{d \ln C}{dx^{6/5}}\right)^{-5/3} \left(\frac{4D_v}{t}\right)^{1/2} \quad [3]$$

where  $\delta$  and  $D_{\text{gb}}$  are the grain boundary width and the grain boundary diffusion coefficient. The curves calculated from Eq. [3] are shown in Fig. 2.

The  $D_v$  and  $D_{\text{gb}}$  are plotted in Fig. 3 as a function of the reciprocal temperature. It is assumed that the effective width  $\delta$  of the twin boundaries is equal to  $3 \times 10^{-10}$  m (16). The temperature dependence of  $^{18}\text{O}$  diffusion is calculated as follows. For lattice diffusion,

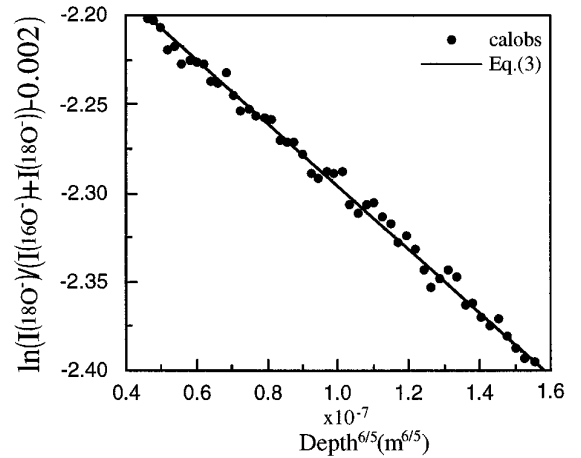


FIG. 2. The diffusion profile of  $^{18}\text{O}$  along the high diffusivity path obtained from a single-crystal  $\text{CaTiO}_3$  annealed at 1121 K for 900 s. The circles show the experimental data, while the solid line is the least-squares fit to Eq. [3].

$$D_v = 9.9^{+74.2}_{-8.7} \times 10^{-2} \exp(-384.5 \pm 21.9 [\text{kJ/mol}]/RT) [\text{m}^2/\text{s}]. \quad [4]$$

For the diffusion along twin boundaries,

$$D_{\text{gb}} = 1.8^{+1.1}_{-0.7} \times 10^6 \exp(-369.2 \pm 4.9 [\text{kJ/mol}]/RT) [\text{m}^2/\text{s}]. \quad [5]$$

The values of  $D_{\text{gb}}$  are 6 to 7 orders of magnitude larger

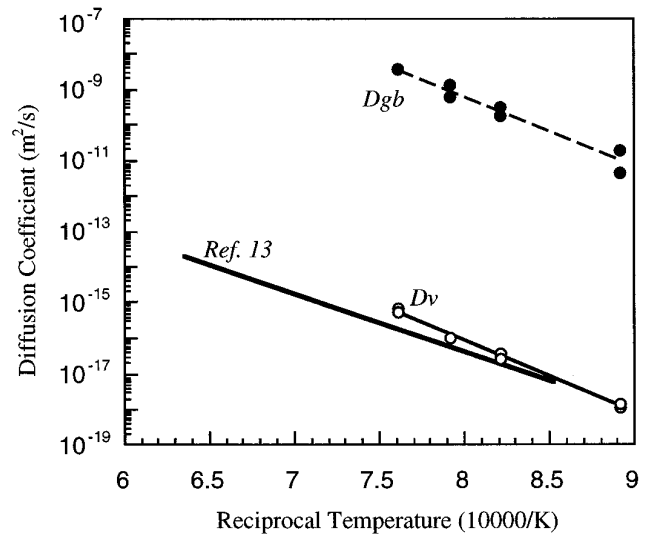


FIG. 3. Arrhenius plot of the diffusion coefficients from  $^{18}\text{O}$  diffusion in the  $b$  direction in single-crystal  $\text{CaTiO}_3$ . The  $D_v$  and  $D_{\text{gb}}$  are the diffusion coefficients obtained from volume and high diffusivity path diffusion. The solid and dotted lines are the least-squares fit to Eqs. [4] and [5]. The large solid line shows the previous result (13).

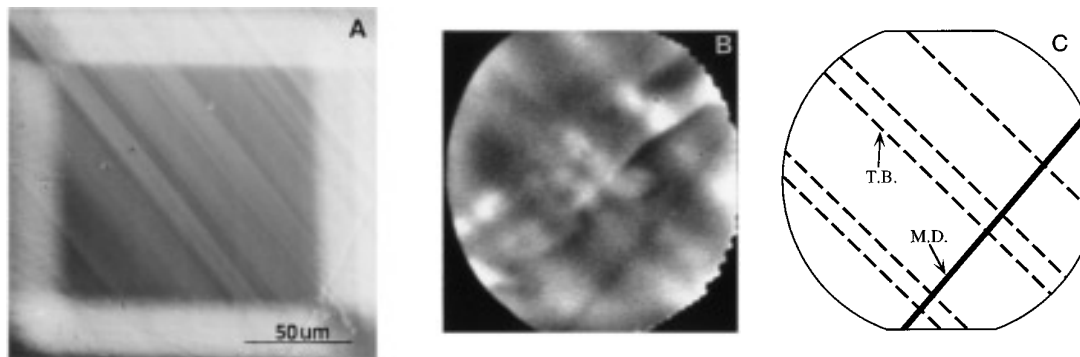


FIG. 4. Optical micrograph,  $^{18}\text{O}^-$  image, and schematic diagram of the  $\text{CaTiO}_3$  surface. (A) is an optical micrograph of the  $\text{CaTiO}_3$  surface. (B) is  $^{18}\text{O}^-$  image at a depth of  $2\ \mu\text{m}$  obtained by SIMS, and its crater is shown in (A). The view field is about  $100\ \mu\text{m}$ . (C) is the schematic diagram of the  $\text{CaTiO}_3$  surface. M.D. and T.B. show the mechanical damage and the twin boundaries.

than those of  $D_v$  at the same temperature. The calculated activation energies for  $D_v$  and  $D_{\text{gb}}$  are in good agreement with each other. The values of  $D_v$  are in good agreement with those previously cited (13), but the activation energy is slightly larger than that previously published.

According to the result in Fig. 1, the large  $^{18}\text{O}$  concentration of the tailing region in the profile suggests the presence of the high diffusivity paths for  $^{18}\text{O}$  diffusion. Figure 4A shows an optical micrograph of the  $\text{CaTiO}_3$  surface. Mechanical damage and the associated microtwinning are observed. There are two reasons that mechanical damage and twin boundaries might act as high diffusivity paths for  $^{18}\text{O}$  diffusion. Previously, it was reported that the tailing region in the profile could occur by mechanical damage (subgrain boundaries and dislocations) introduced by mechanical polishing (17, 18). Microtwinning in  $\text{CaTiO}_3$  was developed by a reversible transition at  $\sim 1573\ \text{K}$  (10, 11) when a single crystal was synthesized by the floating zone method. (The heat treatment for samples in this study was carried out below the transition temperature.) However, there is no evidence linking the high diffusivity path to the twin boundary at this time.

In order to determine the dominant mechanism of the tailing region in the  $^{18}\text{O}$  diffusion profile, the  $^{18}\text{O}^-$  image at a depth of  $2\ \mu\text{m}$  in the crater bottom in Fig. 4A was measured by using a resistive anode encoder (RAE) of SIMS. The  $^{18}\text{O}^-$  image is shown in Fig. 4B, and the pixel brightness is proportional to the  $^{18}\text{O}^-$  intensity. High diffusivity paths for  $^{18}\text{O}$  diffusion are observed. Figure 4C shows the schematic diagram of the distribution of microtwinning and mechanical damage exhibited in Fig. 4B. It is found

that the twin boundary acts as the high diffusivity path of  $^{18}\text{O}$  diffusion at this depth. This result suggests that the tailing region in the  $^{18}\text{O}$  diffusion profile occurs by diffusion along twin boundaries.

## REFERENCES

1. T. Ishigaki, S. Yamauchi, J. Mizusaki, K. Fueki, and H. Tamura, *J. Solid State Chem.* **54**, 100 (1984).
2. T. Ishigaki, S. Yamauchi, K. Kishio, J. Mizusaki, and K. Fueki, *J. Solid State Chem.* **73**, 179 (1988).
3. J. A. Kilner and R. J. Brook, *Solid State Ionics* **6**, 237 (1982).
4. J. Mizusaki, *Solid State Ionics* **52**, 79 (1992).
5. S. Carter, A. Selcuk, R. J. Chater, J. Kajda, J. A. Kilner, and B. C. H. Steele, *Solid State Ionics* **53-56**, 597 (1992).
6. A. Belzner, T. M. Gur, and R. A. Huggins, *Solid State Ionics* **57**, 327 (1992).
7. C. B. Alcock, R. C. Dochi, and Y. Huggins, *Solid State Ionics* **51**, 281 (1992).
8. T. Inoue, J. Kamimae, M. Ueda, K. Eguchi, and H. Arai, *J. Mater. Chem.* **3**, 751 (1993).
9. S. Sasaki, C. T. Prewitt, and J. D. Bass, *Acta Crystallogr. Sect. C* **43**, 1667 (1987).
10. T. J. White, R. L. Segall, J. C. Barry, and J. L. Hutchison, *Acta Crystallogr. Sect. B* **41**, 93 (1985).
11. L. P. Keller and P. R. Buseck, *Am. Miner.* **79**, 73 (1994).
12. N. Doukhan and J. C. Doukhan, *Phys. Chem. Miner.* **13**, 403 (1986).
13. B. Gautason and K. Muehlenbachs, *Science* **260**, 518 (1993).
14. J. Crank, "The Mathematics of Diffusion" Chap. 3.3. Oxford Univ. Press, London, 1975.
15. A. D. Le Claire, *Br. J. Appl. Phys.* **14**, 351 (1963).
16. A. Atkinson and R. I. Taylor, *Philos. Mag. A* **39**, 581 (1979).
17. I. Sakaguchi, H. Yurimoto, and S. Sueno, *Solid State Commun.* **84**, 889 (1992).
18. I. Sakaguchi, H. Haneda, A. Watanabe, and J. Tanaka, submitted for publication.